CoFe-based amorphous alloy with high relaxation frequency

I. Betancourt[a)]
Departamento de Materiales Metalicos y Ceramicos, Instituto de Investigaciones en Materiales, Universidad Nacional Autónoma de México, Mexico DF CP 04510

F. Vazquez
Universidad Tecnológica Tula-Tepeji, Tula de Allende Hidalgo 42800, Mexico

(Received 4 September 2006; accepted 20 December 2006; published online 14 March 2007)

Amorphous $Co_{43}Fe_{20}B_{31.5}Ta_{5.5}$ ribbons prepared by melt-spinning technique, showed a relaxation frequency f_x of 3 MHz, higher than any other known amorphous alloy. Additional complex permeability measurements reflected the reversible bulging of domain walls as the active magnetization mechanism below f_x. The magnetoimpedance (MI) effect was also detected for this alloy, with a maximum variation of 1.6% at 5 MHz. A positive saturation magnetostriction of 0.085×10^{-6} was estimated from tension-stress–MI measurements. © *2007 American Institute of Physics*. [DOI: 10.1063/1.2464189]

I. INTRODUCTION

Cobalt-iron-based amorphous ribbons have attracted considerable interest since long ago due to their particular combination of excellent magnetic and mechanical properties which affords their application in magnetic heads, power supplies, high frequency devices, and various electronic appliances.[1–3] Their magnetic properties depend not only on initial composition and further processing, but also on the alloy final shape (ribbon, wire, glass-covered microwire, thin film, and bulk alloy[4–8]). For instance, the shape of the alloy influences the magnetic anisotropy and the internal stress distributions, and thus the magnetic domain configuration, which in turn determines the frequency-dependent properties, such as the magnetoimpedance (MI) effect.[9] This MI effect refers to variations of the material impedance response as a result of an applied dc magnetic field H_{dc}. The MI phenomenon has been intensively studied since its discovery in numerous soft magnetic materials.[9] On the other hand, high permeability bulk amorphous CoFeTaB alloys have been recently reported to exhibit unique mechanical properties (including fracture strength over 5000 MPa and Young's modulus of 268 GPa).[10] In this work, we present a study of low frequency magnetic properties alongside the stress-dependent MI effect on melt spun CoFeTaB alloys.

II. EXPERIMENTAL TECHNIQUES

Alloy ribbons of composition $Co_{43}Fe_{20}B_{31.5}Ta_{5.5}$ were prepared by means of a chill block melt-spinning technique using a roll speed of 30 m/s, from an ingot previously obtained by arc melting of commercial grade constituents within inert Ar atmosphere. Microstructure features were monitored by x-ray diffraction (XRD) and transmission electron microscopy (TEM) analyses. Complex permeability measurements were carried out on ribbon samples of 1.6 mm width, 8 μm thickness, and 85 mm length by means of an HP 4192A impedance analyzer, with a longitudinal h_{ac}^{long} field of 3 A/m (rms) applied *along* the ribbon length axis with a small solenoid of 100 turns at frequencies within the range of 10 Hz–13 MHz. For the magnetic ac field *transverse* to the ribbon length h_{ac}^{trans} an i_{ac} current of 3.6 mA (rms) was applied along the ribbon main axis at the same frequency range, whereas for MI experiments, an i_{ac} current of 14 mA (rms) was employed at a fixed frequency of 5 MHz, together with a static H_{dc} field between −10 and +10 Oe, generated by means of a 200 turn solenoid powered by a dc source. The saturation magnetization was determined by means of vibrating sample magnetometry (VSM) with a maximum applied field of 400 kA/m.

III. RESULTS AND DISCUSSION

The amorphous microstructure of the $Co_{43}Fe_{20}B_{31.5}Ta_{5.5}$ alloy ribbon was confirmed by XRD and TEM observations, for which Fig. 1 shows a broad maximum together with an image with a modulated contrast and a diffuse halo as diffraction pattern, all of them characteristic features of the amorphous state. The *M-H* curve for this alloy is displayed in Fig. 2. A very thin hysteresis area is observed, reflecting the alloy soft magnetic character. The saturation magnetization M_s was determined as M_s=433 kA/m from the curve, together with a coercivity of 1 kA/m. On the other hand, the spectroscopic $\mu_{re}(f)$ and $\mu_{im}(f)$ plots corresponding to longitudinal and transverse magnetic ac fields are shown in Fig. 3. For $f<1$ MHz, μ_{re} exhibits a constant tendency for both cases, with $\mu_{re}^{long}=1600$ and $\mu_{re}^{trans}=2600$ [Fig. 3(a)]. According to the complex permeability formalism[11] such behavior in μ_{re} can be associated with the reversible bulging of magnetic domain walls, which in turn characterizes the material initial permeability. For increasing f values, a relaxation-type dispersion takes place in both cases, indicating that reversible bulging of domain walls is no longer active as a magnetization mechanism. For $f>5$ MHz, only the spin rotation process is able to follow the variations of the excitation fields h_{sc}^{long} and h_{ac}^{trans} due to its smaller time

[a)]Author to whom correspondence should be addressed; FAX: +52 56161371; electronic mail: israelb@correo.unam.mx

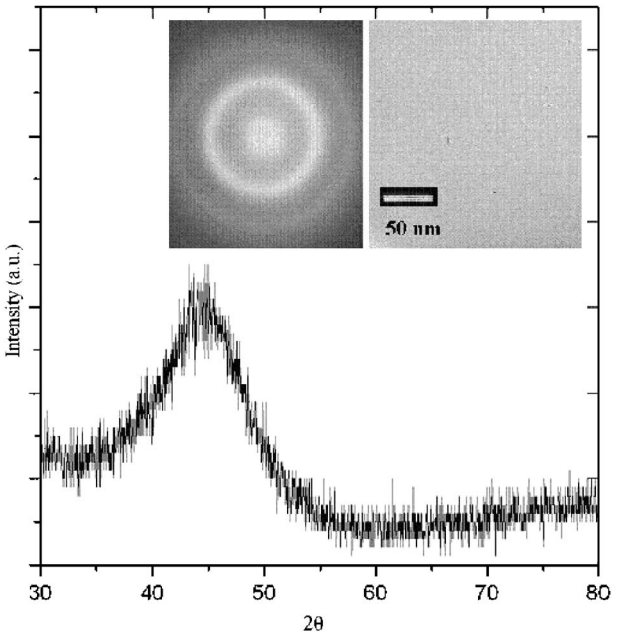

FIG. 1. XRD diffractogram and TEM image for the amorphous $C_{43}Fe_{20}B_{31.5}Ta_{5.5}$ alloy ribbon.

constant compared with reversible bulging. The decrease of both $\mu_{re}^{long}(f)$ and $\mu_{re}^{trans}(f)$ to a nonzero value at this f regime represents the contribution of the spin rotation mechanism to μ_{re}. For the imaginary component of permeability [Fig. 3(b)], both plots manifest clear maxima values at $f=3$ MHz. This particular f value corresponds to the relaxation frequency f_x at which the reversible bulging of magnetic domain walls is unactive. It is worth noticing that $f_x=3$ MHz is a rather high value with respect to amorphous Fe-based alloys [$f_x=0.3-0.5$ MHz (Refs. 12 and 13)] and other CoFe-based alloys [$f_x=0.5-0.8$ MHz (Refs. 14 and 15)] and is comparable to some high frequency Ni–Zn and Zn–Mn ferrites [$f_x=1.0-3.4$ MHz (Refs. 16 and 17)]. The marked difference between μ_{re}^{long} and μ_{re}^{trans} results from a distribution of the magnetic domain directions, which can be oriented parallel, perpendicular, and even oblique to the ribbon axis (this complex distribution of magnetic domains is a consequence of the magnetoelastic coupling during the solidification process[18]). The predominant presence of transverse domains (i.e., perpendicular to the ribbon axis) is evidenced by $\mu_{re}^{trans}>\mu_{re}^{long}$ and by the existence of MI response, as described in the following.

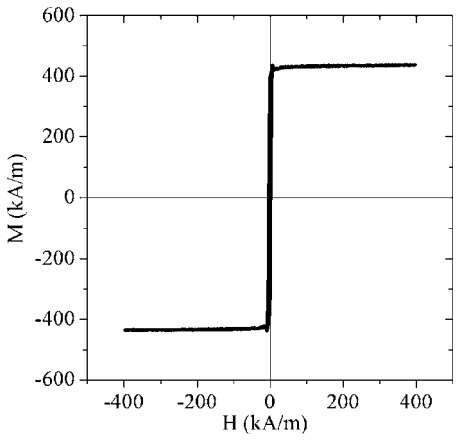

FIG. 2. *M-H* curve for the amorphous $Co_{43}Fe_{20}B_{31.5}Ta_{5.5}$ alloy ribbon.

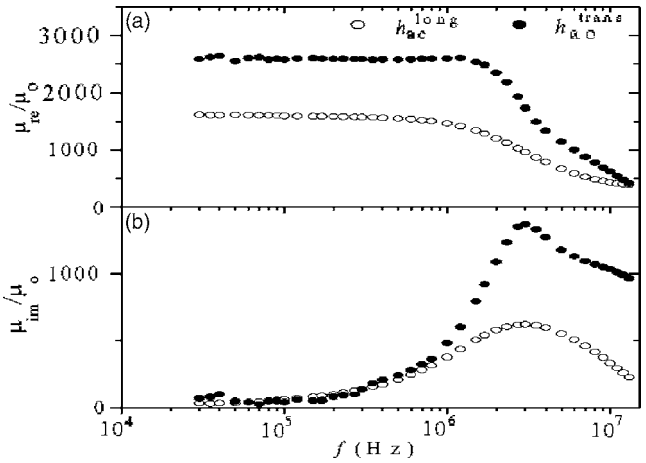

FIG. 3. Spectroscopic $\mu_{re}(f)$ and $\mu_{im}(f)$ plots corresponding to longitudinal and transverse magnetic ac fields for the amorphous $Co_{43}Fe_{20}B_{31.5}Ta_{5.5}$ alloy ribbon.

The MI effect was detected for the present alloy through the MI ratio (defined as $\Delta Z/Z(\%)=100^{*}[Z_{tot}(H)-Z_{tot}(H_{max})]/Z_{tot}(H_{max})$ (Fig. 4), which was measured at $f=5$ MHz$>f_x$ in order to ensure the spin rotation as a magnetization mechanism and thus the evaluation of the alloy's transverse anisotropy field.[8,9] At higher frequencies ($f>5$ MHz) minor MI (H_{dc}) variations were observed, in accordance with equivalent measurements carried out in similar FeCoSiB amorphous alloys,[19] for which the influence of the ferromagnetic resonance effect on the MI response begins at $f>1.5$ GHz, well beyond our equipment limit. For the present $Co_{43}Fe_{20}B_{31.5}Ta_{5.5}$ alloy, the MI ratio exhibits the well known MI double-peak feature[9,11] and a maximum of 1.6%. This rather low MI ratio can be attributed to the distribution of the alloy anisotropy observed in this alloy, rather than a well defined transverse anisotropy. This anisotropy distribution allows the formation of both transverse and parallel magnetic domains (evidenced by the existence of μ_{re}^{long} and μ_{re}^{trans} responses, Fig. 3). In contrast, a

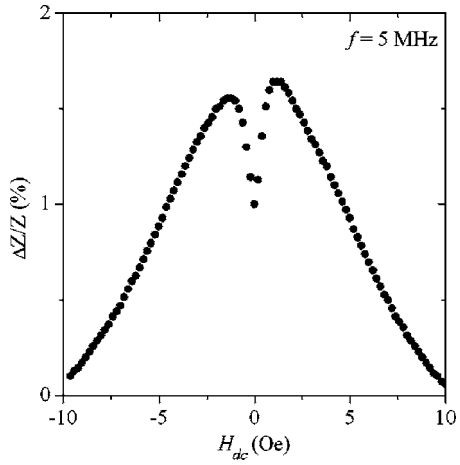

FIG. 4. MI ratio $\Delta Z/Z$ (%) as a function of H_{dc} for the amorphous $Co_{43}Fe_{20}B_{31.5}Ta_{5.5}$ alloy ribbon.

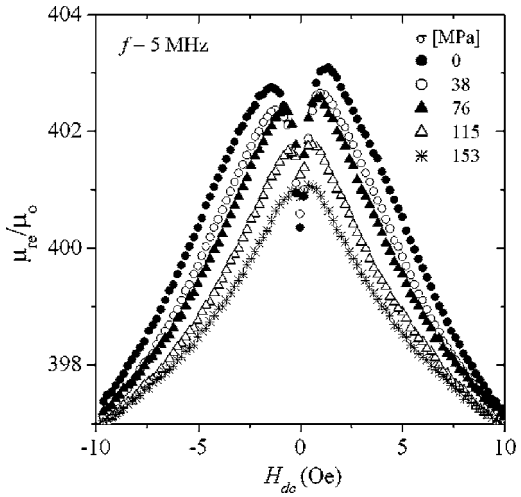

FIG. 5. Real component of permeability as a function of H_{dc} and applied stress.

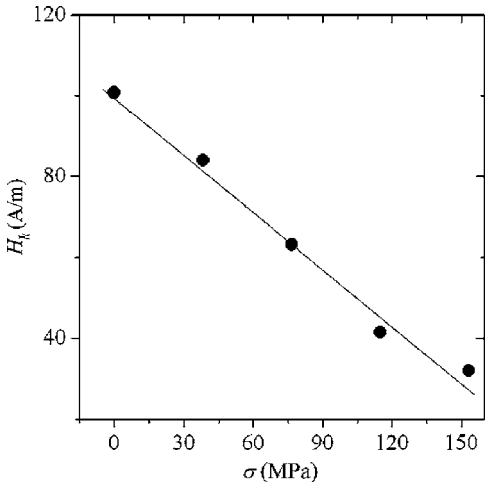

FIG. 6. Dependence of the anisotropy field H_k on the applied stress σ. The solid line corresponds to the linear fitting $H_k=100$ A/m-0.47×10^{-6} A/mPa σ.

key requirement for achieving high MI ratios is a well defined transverse anisotropy (with respect to the i_{ac} flow, coincident with the ribbon axis in this case)[8,9,20] which, in turn, can be attained by suitable stress or magnetic field annealing, as have been demonstrated for amorphous ribbons,[20] wires,[21,22] and thin films.[23]

On the other hand, the maximum values observed for the MI ratio are a consequence of the variation of the skin depth δ, which is inversely proportional to the rotational permeability μ_{rot}, according to $\delta=(2\rho/\omega\mu_{rot})^{1/2}$ (where ρ =resistivity and ω=angular frequency),[9,11] as discussed in the following.

A more physical insight into the MI phenomenon can be described in terms of the complex permeability formalism, from which the complex impedance $\mathbf{Z}=Z_{re}+jZ_{im}[j=(-1)^{1/2}]$ can be transformed into complex permeability $\boldsymbol{\mu}=\mu_{re}+j\mu_{im}$ by means of the relation $\boldsymbol{\mu}=G(-\mathbf{Z}j/\omega)$ with G an appropriate geometrical factor and ω the angular frequency.[11] At $f=5$ MHz, the spin rotation remains as the only magnetization mechanism [since f_x was located at 3 MHz, Fig. 3(b)], and thus the real component of permeability shown in Fig. 5 as a function of H_{dc} and the applied stress corresponds to the rotational permeability. For the stress-free curve, the initial increase of μ_{re}^{rot} can be ascribed to an additional component (axially oriented) of μ_{re}^{rot} exerted by H_{dc}, which results in higher permeability values and thus lower δ values, which in turn lead to increasing Z_{tot} (Fig. 4). The maximum in μ_{re}^{rot} is a consequence of a competition effect in the rotational magnetization process between the axial H_{dc} and the transverse anisotropy field H_k induced during the ribbon fabrication.[18,24] Thus, the maximum appears at $H_{dc}=H_k$.[8] For increasing H_{dc} (>5 Oe), the rotational permeability decreases since the magnetic spins are mostly axially oriented. Consequently, the skin depth increases and thus Z_{tot} decreases gradually as H_{dc} increases (Fig. 4). When increasing stress σ is applied along the ribbon axis, a reduction of H_k is observed (i.e., maximum values closer to 0, Fig. 5) as a result of a progressively higher induced axial anisotropy, which decreases the transverse anisotropy and thus the as-cast transverse magnetoelastic coupling. This behavior is indicative of a positive saturation magnetostriction constant λ_s. The dependence of H_k on σ is displayed in Fig. 6, for which a linear trend is manifested following the relation $H_k=100$ A/m-0.47×10^{-6} A/mPa σ. From this relation it is possible to estimate that λ_s according to[25]

$$\lambda_s=-\left(\frac{\mu_o M_s}{3}\right)\left(\frac{\Delta H_z}{\Delta\sigma}\right), \tag{1}$$

where M_s is the saturation magnetization and ΔH_z corresponds to the variations of the transverse field H_z necessary to compensate the magnetoelastic contribution induced by σ. This equation is proposed for both positive and negative λ_s values.[25] For the present MI measurements, the compensating ΔH_z field corresponds to straightforward H_k. Therefore, Eq. (1) becomes

$$\lambda_s=-\left(\frac{\mu_o M_s}{3}\right)\left(\frac{\Delta H_k}{\Delta\sigma}\right). \tag{2}$$

Taking $\mu_o=12.56\times10^{-7}$ H/m, $M_s=433$ kA/m (Fig. 2), and $\Delta H_k/\Delta\sigma$ as the slope of the $H_k(\sigma)$ plot (Fig. 6), we have $\lambda_s=0.085\times10^{-6}$, in good agreement with the absolute value of λ_s of other CoFe-based alloys.[5,22,26]

IV. CONCLUSIONS

Reversible bulging of magnetic domains was determined as a low frequency magnetization mechanism in amorphous $Co_{43}Fe_{20}B_{31.5}Ta_{5.5}$ ribbons with a high relaxation frequency of 3 MHz, which is comparable to that of some high frequency ferrites. The magnetoimpedance effect was observed in this alloy (with MI ratio of up to 1.6%) together with a vanishing positive magnetostriction constant.

ACKNOWLEDGMENTS

The author acknowledges research funding through Project No. IN119603-UNAM and helpful technical assistance from C. Flores and L. Baños.

[1]R. Hasegawa, J. Magn. Magn. Mater. **100**, 1 (1991).
[2]H. Warlimont and R. Boll, J. Magn. Magn. Mater. **26**, 97 (1982).
[3]M. E. McHenry, M. A. Willard, and D. E. Laughlin, Prog. Mater. Sci. **44**, 291 (1999).
[4]A. Inoue, *Bulk Amorphous Alloys: Practical Characteristics and Applications* (Trans Tech, Switzerland, 1999), pp. 47–57.
[5]P. T. Squire, D. Atkinson, M. R. J. Gibbs, and S. Atalay, J. Magn. Magn. Mater. **132**, 10 (1994).
[6]M. Vazquez, Physica B **299**, 302 (2001).
[7]S. A. Baranov, J. Magn. Magn. Mater. **266**, 278 (2003).
[8]L. V. Panina, K. Mohri, T. Uchiyama, and M. Noda, IEEE Trans. Magn. **31**, 1249 (1995).
[9]M. Knobel, M. Vazquez, and L. Kraus, *Handbook of Magnetic Materials* (Elsevier Science, Holland, 2003), Vol. 15.
[10]A. Inoue, B. L. Shen, H. Koshiba, H. Kato, and A. R. Yavari, Acta Mater. **52**, 1631 (2004).
[11]R. Valenzuela, J. Alloys Compd. **369**, 40 (2004).
[12]J. T. S. Irvine, E. Amano, and R. Valenzuela, Mater. Sci. Eng., A **133**, 140 (1991).
[13]M. Carara, M. N. Baibich, and R. L. Sommer, J. Appl. Phys. **91**, 8441 (2002).
[14]I. Betancourt and R. Valenzuela, IEEE Trans. Magn. **33**, 3973 (1997).
[15]V. M. Prida, M. L. Sanchez, B. Hernando, P. Gorria, M. Tejedor, and M. Vazquez, Appl. Phys. A: Mater. Sci. Process. **A77**, 135 (2003).
[16]J. T. S. Irving, A. R. West, E. Amano, A. Huanosta, and R. Valenzuela, Solid State Ionics **40/41**, 220 (1990).
[17]E. Carrasco, K. L. Garcia, and R. Valenzuela, IEEE Trans. Magn. **34**, 1159 (1998).
[18]M. Vazquez, W. Fernengel, and H. Kronmuller, Phys. Status Solidi A **80**, 195 (1983).
[19]J. M. Barandiaran, A. Garcia-Arribas, and D. de Cos, J. Appl. Phys. **99**, 103904 (2006).
[20]R. L. Sommer and C. L. Chien, Appl. Phys. Lett. **67**, 857 (1995).
[21]D. X. Chen, L. Pascual, and Y. F. Li, J. Magn. Magn. Mater. **218**, L5 (2000).
[22]L. Kraus, M. Vazquez, and A. Hernando, J. Appl. Phys. **76**, 5343 (1994).
[23]R. L. Sommer and C. L. Chien, Appl. Phys. Lett. **67**, 3346 (1995).
[24]G. Bertotti, E. Ferrara, F. Fiorillo, and P. Tiberto, Mater. Sci. Eng., A **226–228**, 603 (1997).
[25]A. Hernando, M. Vazquez, and V. Madurga, J. Magn. Magn. Mater. **37**, 161 (1983).
[26]T. O'Dell, Phys. Status Solidi A **68**, 221 (1981).